MoO_X and WO_X based hole-selective contacts for wafer-based Si solar cells

Stephanie Essig[1], Julie Dréon[1], Jérémie Werner[1], Philipp Löper[1],
Stefaan De Wolf[2], Mathieu Boccard[1], Christophe Ballif[1]

[1] École Polytechnique Fédérale de Lausanne (EPFL), Institute of Microengineering (IMT),
Photovoltaics and Thin-Film Electronics Laboratory, Neuchâtel, Switzerland
[2] King Abdullah University of Science and Technology (KAUST), Thuwal, Saudi Arabia

Abstract — **Highly-transparent carrier-selective front contacts open a pathway towards entirely dopant free Si solar cells. Hole-selective a-Si:H/MoO_x/ITO front contact stacks were already successfully applied in such novel devices. However, for optimum device performance, further improvements are required: We evaluate the use of the high-work-function material WO_X as a replacement for MoO_x in an attempt to reduce optical absorption losses. In addition, we investigate the use of thin hydrogenated SiO_X instead of a-Si:H, and the impact of the residual pressure for MoO_x evaporation.**

Index Terms — **Silicon heterojunction solar cell, carrier-selective contacts, transition metal oxides**

I. INTRODUCTION

The development of dopant-free Si solar cells in which carrier extraction is provided by electron and hole transport layers (ETL and HTL), integrated into passivating contacts, is a promising route to reach efficiencies close to 27% [1]. A typical carrier-selective contact employs a broadband optically transparent material which provides both a chemical passivation of Si surface states and a high (low) work function, inducing in dark and at equilibrium an electrical potential at the Si wafer surface, yielding hole (electron) collection.

A fully doping-free cell with efficiency of 19.4% was realized in ref. [2] by employing a transparent MoO_X-based hole-selective contact on the front side and a LiF-based electron-selective stack on the rear side of an n-type Si wafer. As MoO_X and LiF themselves do not passivate electronic defects at the c-Si surface, thin ~5 nm thick intrinsic hydrogen-rich amorphous silicon (i)a-Si:H interlayers have to be inserted to achieve a high V_{OC}. Our present research aims to further optimize the hole-selective front contact, as already used in ref. [2] and [3]. The motivation for this is that the proposed (i)a-Si:H/MoO_X/ITO front contact stack comes with an important drawback: parasitic light absorption [3] in both the MoO_X, mainly due to transparent conductive oxide (TCO) sputter-induced damage [4], and the ~5 nm thick (i)a-Si:H layer. Furthermore, MoO_X based contact stacks suffer from a fill factor degradation upon annealing at 190°C [5], required for curing of screen printed contacts. This effect could recently be attributed to the release of hydrogen from adjacent layers [6]. In our experiments, we evaluated the possible replacement of MoO_X by WO_X layer. WO_X provides a high work function similar to MoO_X [7, 8] but has a higher transparency both before and after TCO sputter-deposition [4]. Furthermore we tested the impact of the residual base pressure in the evaporation chamber on the performance of solar cells with MoO_X-based front contacts and investigated the use of thermal silicon oxide as an alternative passivation layer with higher transparency and improved thermal resilience.

II. EXPERIMENTAL

Float-zone (100) Si wafers with a thickness of 240 μm and resistance of 3 Ωcm (n-type) were textured and cleaned. For solar cell (Fig. 1a) fabrication, 5-nm-thick (i)a-Si:H layers were applied on the front and rear sides by plasma enhanced chemical vapor deposition (PECVD). On the rear side an about 10 nm thick phosphorous doped a-Si:H layer was deposited in the same tool. After loading in an evaporation chamber, an either ~7-nm-thick MoO_X (x<3) or 5-nm-thick WO_X (x< 3) layer was deposited on the wafer front side by thermal evaporation using stoichiometric powder (MoO_3 or WO_3). Then, 2-cm^2-sized pads of ITO or IZO/ITO were sputter-deposited on the front side and a full-area ITO/Ag rear contact stack was applied. Front metal grids were deposited by Ag screen-printing and cured 20 minutes at 190 °C.
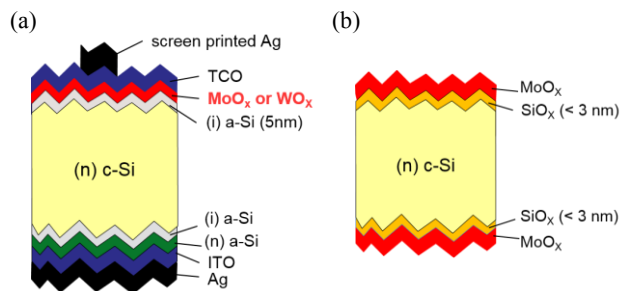

Fig. 1. Schematic sketches of (a) our solar cells with MoO_x or WO_x based hole selective front contact, (b) symmetrical structure to test silicon-oxide buffer layers.

Symmetrical test structures (Fig. 1b) were fabricated to evaluate the passivation of thin thermal silicon oxide layers (1.5-2.5 nm) as buffer layers underlying the MoO_X. For this, textured 200 μm thick (100) n-type Si wafers (~2 Ωcm) and double side polished (DSP) (100) n-type Si wafers (280 μm, ~3 Ωcm) were cleaned in standard wet-chemical solutions. Thin thermal oxide layers were grown in a Rapid Thermal Processing (RTP) furnace using different peak temperatures T_{peak} and oxidation times. Part of the samples were hydrogenated *in-situ* by a Forming Gas Annealing (FGA) process (30 min, 500 °C). Afterwards, all wafers were loaded in a vacuum chamber to evaporate MoO_X layers which had on glass thicknesses of about 15 nm. Finally, the minority carrier lifetimes were determined by QSSPC (Quasi Steady State Photo Conductance) measurements.

III. CELLS WITH WO_X BASED FRONT CONTACTS

Figure 3 shows the JV-curve of our so far best cell with WO_x-based hole-selective contact and its comparison to a cell with an unoptimized MoO_x-based contact fabricated in the same evaporation chamber at low base pressures (10^{-6} mbar). In both cases, sputtered IZO [9] was used as the front TCO layer, deposited in the same chamber immediately after the MoO_X or WO_X thermal evaporation without breaking the vacuum. The cells were characterized after annealing the screen-printed Ag front contact at 190°C. Even though the WO_X based cell achieves a higher short-circuit current density J_{SC}, its V_{OC} equals only 638 mV (Table 1) compared to 705 mV for the MoO_X based cell. Both cells suffer from an S-shaped JV-curve close to the V_{OC}, leading to fill factors of only 70% (WO_X) and 73% (MoO_X). Increasing the WO_X thickness leads to an even stronger S-shape and further reduction in FF (data not shown here). Most likely, the observed low V_{OC} and efficiencies of cells with WO_X based front contact are due to an insufficient band bending provided by our thermally evaporated WO_X material, as discussed in ref. [10].
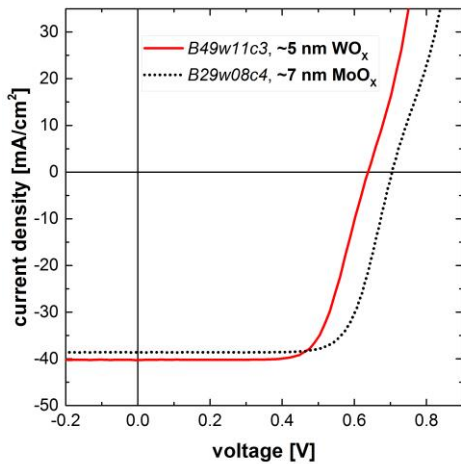

Fig. 2. Light JV-curves of solar cells with MoO_x and WO_X based hole-selective front contact measured after annealing at 190 °C

Table 1. JV parameters of cells of the cells with MoO_X and WO_X based hole-selective contacts from Figure 2.

cell-ID	V_{oc} [mV]	J_{sc} [mA/cm^2]	FF [%]	eff. [%]
B29w08c4, ~7nm MoO_x	705	38.6	72.8	19.8
B49w11c3, ~5nm WO_x	638	40.2	70.1	18.0

IV. IMPACT OF BASE PRESSURE ON MoO_X BASED CONTACTS

Figure 2 compares JV curves of cells with MoO_X-based hole-selective front contacts in which the MoO_X layers were evaporated in vacuum chambers pumped down to different base pressures. We specifically investigated the influence of the water partial pressure by comparing results using a tool equipped with a glovebox and a transfer chamber as a water-free deposition tool (labelled N_2), and a tool opened to air before pumping down (thus with most residual pressure being water vapor, labelled as H_2O). Pumping times were adjusted in both tools to reach a base pressure around 10^{-5} mbar (labelled high p) or 10^{-6} mbar (labelled low p). ITO was then sputter-deposited on all samples, a silver grid was screen printed, and samples were cured at a low temperature of 130 °C. All JV curves show very similar V_{OC} and J_{SC}. A slight S-shape is observed in all cases, yet much more pronounced for the sample prepared with a high base pressure in the tool vented to atmosphere (high p H_2O). This suggests that residual water during evaporation can impact negatively the performance of MoO_X-based devices.
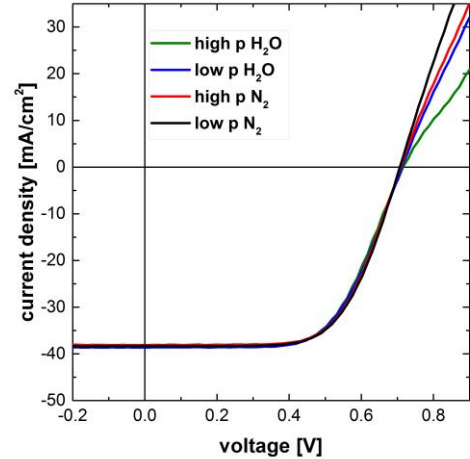

Fig. 3. JV curves of SHJ cells with (i)a-Si:H/MoO_X/ITO hole-selective front contact. The MoO_X layers were deposited after evacuating the chamber to a high (~10^{-5} mbar) or low (10^{-6} mbar) base pressure. MoO_X layers evaporated in the chamber installed in a N2 glovebox lead to superior cell performance compared to those deposited in the chamber which was vented in air before each deposition (labelled "H_2O").

IV. ALTERNATIVE BUFFER LAYERS FOR MoO_X BASED HOLE-SELECTIVE CONTACTS

Figure 4 compares the minority carrier lifetimes of symmetrical test structures with different buffer layers underneath the thermally evaporated MoO_x. The investigated silicon oxide layers were generated by two different recipes leading to oxide thicknesses of 2.0 nm and 2.4 nm, as summarized in Table 2.

The thin thermal oxide layers result in higher lifetimes than achieved with a reference sample that was HF-dipped prior to the MoO_x deposition (no buffer). However their lifetimes of 100 µs to 170 µs at an injection level of 1.10^{15} cm^{-3} are one order of magnitude lower than achieved with an (i)a-Si:H buffer layer (~6 ms). Our data indicate that the surface passivation increases with increasing oxide thickness and hydrogenation. Hydrogenation of the oxide layer 2 (DSP wafer) prior to MoO_x deposition resulted in a higher lifetime (Fig. 4) which translates into an increase in implied V_{OC} (iV_{OC}) from 603 mV to 621 mV. The same effect was observed on textured (TXT) wafers which achieved an iV_{OC} up to 650 mV (hydrogenated oxide 2, Fig. 4).

Further analysis is necessary to investigate the carrier transport in $SiO_X/MoO_X/TCO$ contact stacks and to achieve higher passivation levels comparable to (i)a-Si:H. We expect that there will be a tradeoff between passivation and series resistance for the oxide layer thickness when applied in a real solar cell device.

Table 2. Parameters used for the different rapid thermal oxidations. The oxide thicknesses were determined by spectral ellipsometry on reference DSP Si (100) wafers.

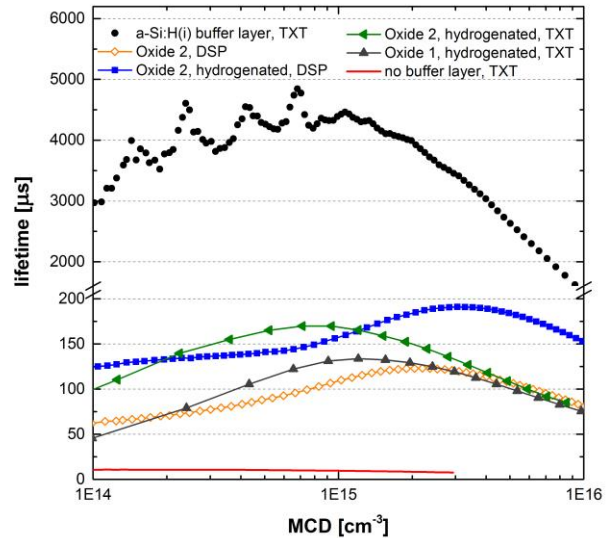| Oxide recipe	T_{peak} [°C]	oxidation time [s]	Oxide thickness measured on DSP [nm]
Oxide 1	700	90	2.0
Oxide 2	750	90	2.4

Fig. 4. Carrier lifetime versus minority carrier density (MCD) of symmetrical test structures (Fig 1b) with different buffer layers as described in the text.

V. CONCLUSION AND OUTLOOK

Our experimental results show that both MoO_X and WO_X can be used in hole-selective contacts. However, so far WO_X-based hole-selective contacts resulted in lower V_{OC}. The performance of a-Si:H/MoO_x/TCO hole-selective contact stacks depends critically on the base pressure and residual water vapor in the deposition chamber. Symmetrical test structures with stacks of 2.4 nm thick hydrogenated SiO_x layers and MoO_x resulted in iV_{OC} of 650 mV. Further investigation is required to evaluate its applicability in a real device and its optimal properties for best performance.

REFERENCES

1. Battaglia, C., A. Cuevas, and S. De Wolf, *High-efficiency crystalline silicon solar cells: status and perspectives.* Energy & Environmental Science, 2016. **9**(5): p. 1552-1576.

2. Bullock, J., et al., *Efficient silicon solar cells with dopant-free asymmetric heterocontacts.* Nature Energy, 2016. **1**: p. 15031.

3. Geissbühler, J., et al., *22.5% efficient silicon heterojunction solar cell with molybdenum oxide hole collector.* Applied Physics Letters, 2015. **107**(8): p. 081601.

4. Werner, J., et al., *Parasitic Absorption Reduction in Metal Oxide-Based Transparent Electrodes: Application in Perovskite Solar Cells.* ACS Applied Materials & Interfaces, 2016. **8**(27): p. 17260-17267.

5. Geissbühler, J., et al., *Silicon Heterojunction Solar Cells With Copper-Plated Grid Electrodes: Status and Comparison With Silver Thick-Film Techniques.* IEEE Journal of Photovoltaics, 2014. **4**(4): p. 1055-1062.

6. Essig, S., et al., *MoO$_X$-based hole-selective contacts for Si photovoltaics: hydrogen-rich layers as fill-factor killers.* submitted.

7. Gerling, L.G., et al., *Transition metal oxides as hole-selective contacts in silicon heterojunctions solar cells.* Solar Energy Materials and Solar Cells, 2016. **145, Part 2**: p. 109-115.

8. Bivour, M., et al., *Molybdenum and tungsten oxide: High work function wide band gap contact materials for hole selective contacts of silicon solar cells.* Solar Energy Materials and Solar Cells, 2015. **142**: p. 34-41.

9. Morales-Masis, M., et al., *Low-Temperature High-Mobility Amorphous IZO for Silicon Heterojunction Solar Cells.* IEEE Journal of Photovoltaics, 2015. **5**(5): p. 1340-1347.

10. Mews, M. et al., *Oxygen vacancies in tungsten oxide and their influence on tungsten oxide/silicon heterojunction solar cells.* Solar Energy Materials & Solar Cells 158, pp. 77–83 (2016).